from excited Ca atoms at temperatures between 725 and 900 K, where the N_2O concentration entering their reactor was in excess over the equilibrium Ca vapor pressure, suggests that most of the N_2O was removed in situ, possibly through a heterogeneous reaction with hot solid Ca. At temperatures between 900 and 1100 K, the Ca vapor pressure would have been in excess over the N_2O. Thus, the time-resolved molecular emission which those workers[25] observed from excited CaO was most likely the result of electronic energy transfer from $Ca(^3P_J,^1D_2)$ to CaO, and the measured rate constants for the quenching of these excited atomic states are for reaction with CaO rather than N_2O.

CaO + O. Although there is some uncertainty regarding the bond energy of CaO,[42] assuming the recent value[42] of $D_0(Ca-O) = 396.5 \pm 6.8$ kJ mol^{-1} indicates that reaction 2 is exothermic by about 101 kJ mol^{-1}. Equation 9 implies that reaction 2 proceeds at the collision number and hence possesses a negligible energy barrier. The temperature dependence of reaction 2 may thus be expressed as[48]

$$k_2(T) = (4.0 \pm 1.3) \times 10^{-10}(T/300)^{1/2} \text{ cm}^3 \text{ molecule}^{-1} \text{ s}^{-1} \quad (13)$$

Although this reaction has not been studied previously, we have observed a similar absence of an energy barrier for the analogous reaction NaO + O.[49]

Mesospheric Implications. We pointed out in the Introduction the atmospheric significance of studying reaction 2, namely, to understand the observed depletion of atomic Ca relative to atomic Na, in the mesosphere at about 90 km. The present result (eq 13) indicates that the reduction of CaO to Ca by atomic O is too rapid for CaO to be a significant reservoir for ablated Ca in the mesosphere. We are therefore proceeding to examine the chemistry of calcium superoxide, CaO_2, as a possible explanation for the low mesospheric abundance of atomic Ca.[28]

Acknowledgment. This work was supported under Grant ATM-8820225 from the National Science Foundation.

Appendix

The reaction CaO + O was studied by photolyzing CaO/N_2O under conditions of excess N_2O, such that the loss of Ca by reaction 1 was rapid and diffusional loss could be neglected. Thus

$$d[Ca]/dt = k_2[CaO][O] - k_1[Ca][N_2O] \quad (A1)$$

$$d[O]/dt = -k_2[CaO][O] \quad (A2)$$

Since both CaO and N_2O are in pseudo-first-order excess over Ca and O

$$d[Ca]/dt = k_2'[O] - k_1'[Ca] \quad (A3)$$

$$d[O]/dt = -k_2'[O] \quad (A4)$$

If $[Ca]_0$ and $[O]_0$ are the concentrations of these atoms formed by the photolysis of CaO and N_2O, and assuming effectively instantaneous quenching of $O(^1D)$ formed from the photolysis of N_2O (see text), then the atomic Ca concentration at time t is given by

$$[Ca] = ([Ca]_0 + k_2'/(k_2' - k_1')[O]_0)\exp(-k_1't) - k_2'/(k_2' - k_1')[O]_0 \exp(-(k_2' - 2k_1')t) \quad (A5)$$

(49) Plane, J. M. C.; Husain, D. *J. Chem. Soc., Faraday Trans. 2* **1986**, *82*, 2047.

Kinetics of the Reaction OH + NH_3 in the Range 273–433 K

Eric Wei-Guang Diau, Tai-Ly Tso, and Yuan-Pern Lee*,†

Department of Chemistry, National Tsing Hua University, 101, Sec. 2, Kuang Fu Road, Hsinchu, Taiwan 30043, R.O.C. *(Received: December 4, 1989; In Final Form: February 21, 1990)*

The kinetics of the reaction OH + NH_3 have been studied by means of the flash photolysis/laser-induced fluorescence technique. The rate of this reaction was investigated in the range 273–433 K under more extensive conditions ($68 < P/\text{Torr} < 504$, $0.29 < [NH_3]/10^{15}$ molecules cm^{-3} < 36.1) than previously. The results from experiments with the Xe lamp and with the KrF laser for photolysis agree well within the experimental uncertainties, indicating the absence of interference due to excess NH_2 which was produced by photolysis with the Xe lamp. A fit of rate coefficients to the Arrhenius equation yields $k = (3.29 \pm 1.02) \times 10^{-12} \exp[-(922 \pm 100)/T]$ cm^3 molecule^{-1} s^{-1}, with $k = (1.47 \pm 0.07) \times 10^{-13}$ cm^3 molecule^{-1} s^{-1} at 297 K; the uncertainties represent one standard error. The rate constant of the interfering reaction, OH + NH_2 → products, was also estimated to be less than 7×10^{-12} cm^3 molecule^{-1} s^{-1}.

Introduction

Although ammonia is a minor constituent of the terrestrial atmosphere, it plays a significant role in both homogeneous and heterogeneous atmospheric reactions.[1,2] Being the dominant basic gas in the atmosphere, ammonia partially neutralizes atmospheric acids in precipitation. On the other hand, NH_3 may be oxidized in the atmosphere to odd-nitrogen species which contribute to the acidity of precipitation.

The rate-determining step in the oxidation of NH_3 is its reaction with hydroxyl radical:

$$OH + NH_3 \rightarrow H_2O + NH_2 \quad (1)$$

The ultimate fate of amidogen radical (NH_2) formed in reaction 1 is not well understood. NH_2 could be a significant source of atmospheric NO_x by its reaction with O_2 or O_3, otherwise a significant sink via the reactions of NH_2 with NO or NO_2. The rates and mechanisms of these potentially important reactions of NH_2 require further studies.[3,4] Similarly, reaction 1 is also important in the conversion of fuel nitrogen to NO_x[5] and in the removal of NO_x from fuel gases in combustion by the addition of NH_3.[6]

† Also affiliated with the Institute of Atomic and Molecular Sciences, Academia Sinica, R.O.C.

(1) McConnell, J. C. *J. Geophys. Res.* **1973**, *78*, 7812.
(2) Wofsy, S. C.; McElroy, M. B. *Can. J. Chem.* **1974**, *52*, 1582.
(3) DeMore, W. B.; Golden, D. M.; Hampson, R. F.; Howard, C. J.; Kurylo, M. J.; Molina, M. J.; Ravishankara, A. R.; Sander, S. P. *JPL Publ.* **1987**, *No. 87-41*.
(4) Westley, F.; Herron, J. T.; Cvetanovic, R. J.; Hampson, R. F.; Mallard, W. G. NIST Chemical Gas Kinetics Database, Ver. 1.1 (*NIST Stand. Ref. Database* **1989**, *17*).
(5) Song, Y. H.; Blair, D. W.; Siminski, V. J.; Bartok, W. *Symp. (Int.) Combust., [Proc.], 18th* **1981**, 53.

0022-3654/90/2094-5261$02.50/0

There have been many kinetic studies of reaction 1 by various techniques.[7-25] The range of the reported rate constant at room temperature is $0.41 < k/10^{-13}$ cm^3 molecule^{-1} s^{-1} < 2.7, whereas the range of the reported Arrhenius activation energy is 438 K $< E/R <$ 4539 K over the temperature range 225–2360 K. Although a current review[3] recommends

$$k_1 = 3.6 \times 10^{-13} \exp[-(930 \pm 200)/T] \quad \text{cm}^3 \text{ molecule}^{-1} \text{ s}^{-1} \tag{2}$$

based on the work of five groups with k_1 in the range (1.44–1.73) $\times 10^{-13}$ cm^3 molecule^{-1} s^{-1}, there are still some problems associated with the kinetic studies of this reaction. First, previous studies using the flash photolysis technique used a Xe lamp instead of lasers; the lamp should generate more NH_2 than OH in the system because of the relatively large photolysis cross section of NH_3, about 200 nm.[26] The effect of excess NH_2 in the reaction cell on the measurement of k_1 has not been thoroughly investigated. The studies using the discharge flow technique also suffered from the interfering reactions between NH_2 (product of reaction 1) and NO_2 (reactant for OH production). Second, previous studies except a few at high temperatures were performed at $P < 35$ Torr. Although the title reaction is expected to be bimolecular and thus to have no pressure dependence, it is still desirable to extend the experimental conditions to investigate possible effects on the rate coefficient due to unthermalized reactant or possible secondary reactions.

We have constructed an experimental system which utilizes either a flash lamp or an UV laser to generate radical reactants and a tunable laser to probe the reactant by the laser-induced fluorescence (LIF) technique in order to study the kinetics of reaction 1. With the laser photolysis arrangement, the problems associated with NH_3 photolysis have been eliminated. Accurate values of the rate coefficient as well as its temperature dependence have been obtained at pressures up to 504 Torr and $273 < T/\text{K} < 433$.

Experimental Section

The experiments were carried out with a typical flash photolysis system which consists of a light source for the generation of OH radicals, a thermostated reaction vessel, and a LIF detection system to monitor the concentration of OH radicals.

When the xenon flash lamp (EG&G, FX-193U) was used, OH radicals were produced by photolysis of H_2O at 0.03–0.15 Torr in the reaction vessel:

$$H_2O + h\nu \ (\lambda \leq 185 \text{ nm}) \rightarrow OH + H \tag{3}$$

Flash energies of 84–635 mJ pulse^{-1} were produced by charging a 1.27-μF capacitor to 364–1000 V. When the excimer laser was employed, OH radicals were generated by photolysis of 0.001–0.003 Torr of H_2O_2 with the radiation from the KrF laser (Lambda Physik, LPX120i):

$$H_2O_2 + h\nu \ (\lambda = 248 \text{ nm}) \rightarrow OH + OH \tag{4}$$

Hydroxyl radicals were detected by the pulsed LIF technique. The frequency-doubled output of a dye laser (Spectra Physics, PDL-2), which was pumped by the second harmonic of a Nd:YAG laser (Spectra Physics, DCR-2A), was directed into the reaction cell perpendicular to the axis of photolysis. The $Q_1(1)$ line of the $A^2\Sigma^+(v'=1) \leftarrow X^2\Pi(v''=0)$ transition at 282.0 nm was chosen for excitation. The $A^2\Sigma(v'=0) \rightarrow X^2\Pi(v''=0)$ fluorescence about 309.6 nm was collected in the direction perpendicular to the excitation and photolysis axes through an interference filter (fwhm 12 nm, 43% transmission at 309.6 nm) and detected by a photomultiplier tube (Hamamatsu, R212 UH). The output of the detector was amplified and averaged by a boxcar integrator (Stanford Research, SR250).

The temporal profile of OH concentration was obtained by varying the time delay between the photolysis pulse and the LIF probe laser pulse. The repetition rates of both light pulses were set at 10 Hz. Typically, 100 pulses of the signal were averaged at each time delay. The triggers for the flash lamp, the lasers, and the boxcar integrator were generated from a pulse generator (Stanford Research, DG535) which was controlled by a microcomputer. The communication among the microcomputer, the pulse generator, and the boxcar integrator was achieved via the IEEE-488 (GPIB) interface using the ASYST (McMillan Co.) software.

The intensity of the OH LIF signal was determined by subtracting the scattered light from the observed total emission. The intensity of the scattered light was measured in each decay measurement by determining the observed emission after the probe laser pulse which was fired after a long delay (98 ms) from the photolysis pulse.

A jacketed reaction cell with an internal volume about 150 cm^3 was used in all experiments. It was maintained at a constant temperature by circulation of ethanol, water, or silicon oil from a thermostated bath (Neslab, RTE-210) through the outer jacket. All experiments were carried out under "slow flow" conditions to replenish reactants. The concentration of each component in the reaction mixture was determined from measurements of the mass flow rates and the total pressure (measured with an MKS Baratron manometer).

Typical experimental conditions were as follows: total flow rate F_T = 2–20 STP cm^3 s^{-1}; total pressure P = 68–504 Torr; reaction

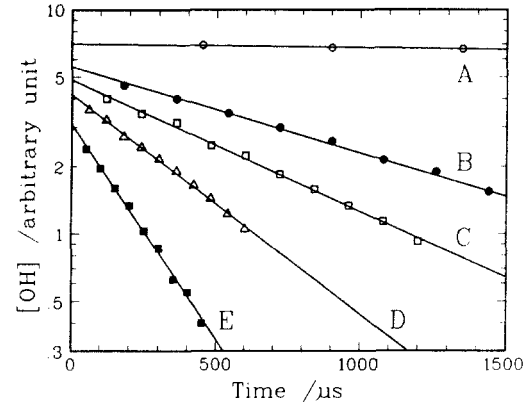

Figure 1. Pseudo-first-order decay of OH for various concentrations of NH_3. T = 433 K, P = 199 Torr, KrF laser photolysis. [NH_3] in molecules cm^{-3}: A, 0; B, 2.1 $\times 10^{15}$; C, 3.3 $\times 10^{15}$; D, 5.5 $\times 10^{15}$; E, 9.4 $\times 10^{15}$.

(6) Lyon, R. K. *Int. J. Chem. Kinet.* **1976**, *8*, 315.
(7) Kurylo, M. J. *Chem. Phys. Lett.* **1973**, *23*, 467.
(8) Stuhl, F. *J. Chem. Phys.* **1973**, *59*, 635.
(9) Dove, J. E.; Nip, W. S. *Can. J. Chem.* **1974**, *52*, 1171.
(10) Hack, V. W.; Hoyermann, K.; Wagner, H. G. *Ber. Bunsen-Ges. Phys. Chem.* **1974**, *78*, 386.
(11) Cox, R. A.; Derwent, R. G.; Holt, P. M. *Chemosphere* **1975**, *4*, 201.
(12) Gordon, S.; Mulac, W. A. *Int. J. Chem. Kinet.* **1975** (Symp. No. 1), 289.
(13) (a) Zellner, R.; Smith, I. W. M. *Chem. Phys. Lett.* **1974**, *26*, 72. (b) Smith, I. W. M.; Zellner, R. *Int. J. Chem. Kinet.* **1975** (Symp. No. 1), 341.
(14) Perry, R. A.; Atkinson, R.; Pitts Jr., J. N. *J. Chem. Phys.* **1976**, *64*, 3237.
(15) Pagsberg, P. B.; Erisksen, J.; Christensen, H. C. *J. Phys. Chem.* **1979**, *83*, 582.
(16) Fenimore, C. P. *Combust. Flame* **1980**, *37*, 245.
(17) Silver, J. A.; Kolb, C. E. *Chem. Phys. Lett.* **1980**, *75*, 191.
(18) (a) Fujii, N.; Miyama, H.; Asaba, T. *Chem. Phys. Lett.* **1981**, *80*, 355. (b) Fujii, N.; Miyama, H.; Koshi, M.; Asaba, T. *Symp. (Int.) Combust., [Proc.], 18th* **1981**, 873.
(19) Niemitz, K. J.; Wabner, H. G.; Zellner, R. *Z. Phys. Chem. (Munich)* **1981**, *124*, 155.
(20) Salimian, S.; Hanson, R. K.; Kruger, C. H. *Int. J. Chem. Kinet.* **1984**, *16*, 725.
(21) Stephens, R. D. *J. Phys. Chem.* **1984**, *88*, 3308.
(22) Zabielski, M. F.; Seery, D. J. *Int. J. Chem. Kinet.* **1985**, *17*, 1191.
(23) Gehring, M.; Hoyermann, K.; Schacke, H.; Wolfrum, J. *Symp. (Int.) Combust., [Proc.], 14th* **1973**, 99.
(24) Jeffries, J. B.; Smith, G. P. *J. Phys. Chem.* **1986**, *90*, 487.
(25) (a) Fujii, N.; Chiba, K.; Uchida, S.; Miyama, H. *Chem. Phys. Lett.* **1986**, *127*, 141. (b) Fujii, N.; Uchida, S.; Sato, H.; Fujimoto, S.; Miyama, H. *Bull. Chem. Soc. Jpn.* **1986**, *59*, 3431.
(26) Watanabe, K. *J. Chem. Phys.* **1954**, *22*, 1564.

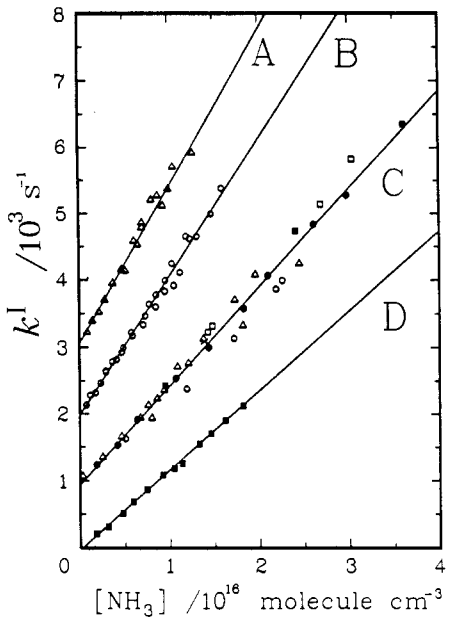

Figure 2. Plots of the pseudo-first-order decay rate k_1 against NH_3 concentration for Xe flash lamp photolysis at various temperatures: A, 363 K (Δ: 315 Torr, 42 mJ); B, 338 K (○: 313 Torr, 42 mJ); C, 297 K (●: 311 Torr, 42 mJ; ○: 486 Torr, 88 mJ; Δ: 486 Torr, 148 mJ; □: 320 Torr, 268 mJ; ×: 417 Torr, 268 mJ; ■: 504 Torr, 268 mJ); D, 273 K (■: 303 Torr, 42 mJ). The origins have been displaced vertically by 3000, 2000, and 1000 s^{-1} for A, B, and C, respectively.

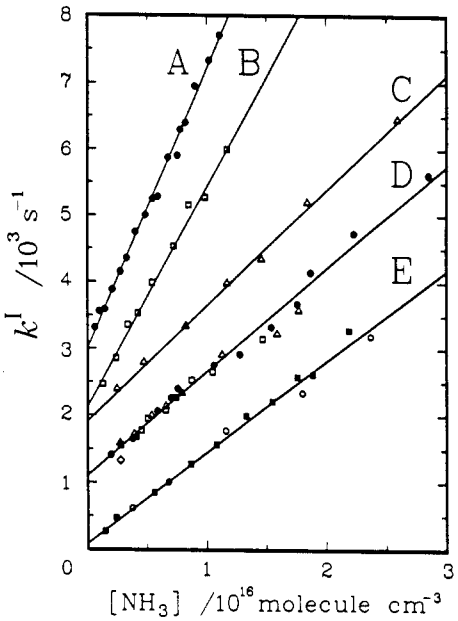

Figure 3. Plots of the pseudo-first-order decay rate k_1 against NH_3 concentration for KrF laser photolysis at various temperatures: A, 433 K (●: 199 Torr, 9 mJ); B, 398 K (□: 263 Torr, 8 mJ); C, 317 K (Δ: 209 Torr, 7 mJ); D, 298 K (●: 111 Torr, 9 mJ; Δ: 68 Torr, 10 mJ; □: 465 Torr, 9 mJ; ■: 465 Torr, 6 mJ; ◇: 465 Torr, 2 mJ); E, 283 K (■: 386 Torr, 8 mJ; ○: 116 Torr, 8 mJ). The origins have been displaced vertically by 3000, 2000, 2000, and 1000 s^{-1} for A, B, C, and D, respectively.

temperature T = 273–433 K; flow velocity v = 1–10 cm s^{-1}; [H_2O] = (1–5) × 10^{15} molecules cm^{-3} or [H_2O_2] ≃ (3–10) × 10^{13} molecules cm^{-3}; [NH_3] = (2.9–361) × 10^{14} molecules cm^{-3}; [OH] ≃ (1–6) × 10^{11} molecules cm^{-3}; time interval between two light sources t = 0.002–40 ms.

The diluent gas He (99.9995%) was used without further purification. Distilled H_2O was thoroughly degassed prior to use. The flow rate of NH_3 (99.99%) was determined by measurement of the rate of pressure change in a calibrated volume. In some experiments a mixture of (11.9 ± 0.3)% NH_3 in He was prepared, and a Tylan mass flowmeter was used to determine the flow rate. The NH_3 concentration of the mixture was determined with a FTIR spectrometer and a 10-cm gas cell. The integrated absorbance of NH_3 at 1538.01, 1567.99, 1667.35, 1701.40, 1731.69, and 1804.40 cm^{-1} from mixtures of known concentrations was used for calibration.

Results and Discussion

The experiments were carried out under pseudo-first-order conditions with [NH_3]/[OH] > 10^3. Thus, the LIF signal of OH after correction for scattered light is expected to exhibit simple exponential decay with respect to reaction time. Figure 1 shows some typical decays of [OH] as a function of reaction time for various concentrations of NH_3 at 433 K. In the absence of NH_3 (trace A), the decay rate reflects the loss of OH due both to diffusion from the viewing zone of the detector and to possible reactions of OH; the most probable reaction of OH is that with the parent molecules

$$OH + H_2O_2 \rightarrow HO_2 + H_2O \quad (5)$$

for which k_5 = 1.7 × 10^{-12} cm^3 $molecule^{-1}$ s^{-1}.[3] Usually the decay rate ranged 50–180 s^{-1} as long as [H_2O_2] and [OH] were not in excess. As NH_3 was added to the reaction cell, the [OH] decay rate increased with [NH_3] (traces B–E). The pseudo-first-order rate constant k^1 was determined from the slope of the logarithmic decay plot for each [NH_3].

$$k^1 = d \ln [OH]/dt \quad (6)$$

Variation of the gate width of the boxcar integrator from 0.48 to 1.2 μs made no change in the value of k^1, indicating that the LIF signal of OH was not saturating the detector and that probably no interfering emission was present. The excellent linearity shown in Figure 1 also indicates that pseudo-first-order decay was well represented; hence secondary reactions were likely negligible.

TABLE I: Summary of Measurements of the Rate Constant of the Reaction OH + NH_3

T, K	P, Torr	[NH_3], 10^{15} molecules cm^{-3}	no. of expts	intercept, s^{-1}	k_1, 10^{-13} cm^3 $molecule^{-1}$ s^{-1}
Photolysis by Means of Xe Flash Lamp					
273	303	1.77–18.2	12	−23 ± 39[a]	1.18 ± 0.03[a]
297	311–504	0.29–36.1	37	−5 ± 75	1.44 ± 0.08
338	313	0.70–15.9	27	4 ± 87	2.04 ± 0.11
363	315	0.84–12.7	17	28 ± 128	2.43 ± 0.12
Photolysis by Means of KrF Excimer Laser					
283	116–386	1.48–23.7	15	98 ± 140	1.36 ± 0.09
298	68–465	1.97–28.5	29	132 ± 89	1.50 ± 0.06
317	209	2.46–25.9	7	−32 ± 227	1.71 ± 0.15
398	263	1.26–11.7	9	69 ± 169	3.44 ± 0.24
433	199	0.62–11.1	17	56 ± 127	4.12 ± 0.11

[a] The uncertainties represent one standard error.

In the experiments using the flash lamp as a photolysis source, a small (~10%) but definite decrease of the rate constant was observed as the pressure was increased from 25 to 300 Torr. The rate coefficient was constant at pressures of 300–500 Torr. An increase in the flash energy from 42 to 268 mJ also increased the observed rate coefficient by about 11% at 90 Torr and less than 5% at 500 Torr. This result suggests that a small fraction of OH produced from the photolysis at high energies and low pressures might not be at thermal equilibrium. Presumably, OH in the excited state reacts with NH_3 at a higher rate than those in the ground state. Most experiments were therefore carried out at smaller photolysis energies and greater pressures.

Figures 2 and 3 show plots of k^1 vs [NH_3] at various temperatures with flash lamp and laser as photolysis source, respectively. The excellent linearity of these lines over a wide range of [NH_3] is clearly illustrated. For experiments with Xe lamp photolysis, the rate coefficient was independent of lamp energy (42–268 mJ) if the pressure of the cell was above 300 Torr, as

TABLE II: Summary of Reported Values of the Rate Constants of the Reaction OH + NH_3 at Temperatures of <500 K[a]

k_1 at room temp, 10^{-13} cm^3 s^{-1} molecule^{-1}	Arrhenius form $A\exp(-E/RT)$						
	$A/10^{-12}$, cm^3 s^{-1} molecule^{-1}	E/R, K	T, K	P, Torr	$[NH_3]$, 10^{14} molecules cm^{-3}	method[b]	investigator
1.47 ± 0.07	3.29 ± 1.02	922 ± 100	273–433	68–504	2.9–361	LP, FP/LIF	this work
0.41 ± 0.06				~25	10–80	FP/RF	Kurylo[7]
1.5 ± 0.4				~20	2–15	FP/RF	Stuhl[8]
1.57	2.3	805	228–472	8–30	160–750	FP/RA	Smith and Zellner[13]
1.64 ± 0.16	2.93	861 ± 151	297–427	~30	3–25	FP/RF	Perry et al.[14]
2.42	5.3 ± 0.8	920	298–669	1.25–2.2	0.3–25	DF/ESR	Hack et al.[10]
1.44 ± 0.29	5.41 ± 0.86	1067 ± 72	294–1075	1.2–1.6	0.15–4.2	DF/RF	Silver and Kolb[17]
1.73 ± 0.11	4.55 ± 1.1	973 ± 78	297–364	~1	1.5–11	DF/RF	Stephens[21]
1.20 ± 0.4				~760	NA[c]	FP/CL	Cox et al.[11]
2.7 ± 0.3	1.1	438 ± 40	298–365	~750	~10^5	PR/RA	Pagsberg et al.[15]

[a] High-temperature studies using the shock tube or the pyrolysis technique are not included. [b] LF, laser photolysis; FP, flash photolysis; DF, discharge flow; PR, pulse radiolysis; LIF, laser-induced fluorescence; RF, resonance fluorescence; RA, resonance absorption; ESR, electron spin resonance; CL, chemiluminescence. [c] Not available.

illustrated in trace C of Figure 2. For experiments with laser photolysis, the rate coefficient was independent of laser energy (2–10 mJ) and pressure (68–465 Torr), as shown in trace D of Figure 3. The slopes of these lines yield the bimolecular rate constants k_1 for reaction 1. Table I presents a summary of the results fitted by least squares and the corresponding experimental conditions at each temperature. At 297 K, k_1 was determined to be 1.44×10^{-13} cm^3 molecule^{-1} s^{-1} from experiments using the Xe lamp for photolysis. At 298 K, k_1 was determined to be 1.50×10^{-13} cm^3 molecule^{-1} s^{-1} from experiments using the laser photolysis technique. The discrepancy (~4%) is well within the experimental uncertainties, and there is no apparent reason to explain the deviation.

H_2O_2 in the reaction cell was maintained at small concentrations so as to minimize both reaction 5 and the self-reaction of OH

$$OH + OH \rightarrow \text{products} \quad (7)$$

for which $k_7 = 1.9 \times 10^{-12}$ cm^3 molecule^{-1} s^{-1}.[3] When excessive OH was present (usually when $[H_2O_2]$ was too great), reaction 7 was not negligible and the logarithmic decay plot showed downward curvature due to the second-order reaction. Thus, before each set of experiments, a blank decay (t up to 40 ms) was determined in the absence of NH_3 to ensure that OH was not in excess. The k^1 for the blank decay was usually in the range 50–180 s^{-1}, indicating a maximum of $(3–10) \times 10^{13}$ molecules cm^{-3} for $[H_2O_2]$ if reaction 5 was assumed to be the major source for the OH decay. Under such experimental conditions, $[NH_3]/[OH] > 10^3$; therefore, the interference due to reaction 7 is less than 1% of the total reaction rate measured.

When the flash lamp was used as a photolytic source, the photolysis of NH_3 also took place:

$$NH_3 + h\nu\ (\lambda < 280\ \text{nm}) \rightarrow NH_2 + H \quad (8)$$

In the region near 200 nm, the absorption cross section of NH_3 has been determined to be $(4–20) \times 10^{-18}$ cm^2 with a quantum yield near unity for the production of the NH_2 in the ground electronic state.[26] Because as much as 0.2% of NH_3 was photolyzed in the flash lamp experiments, the reaction

$$OH + NH_2 \rightarrow \text{products} \quad (9)$$

could be important. The rate constant of reaction 9 has been estimated to be $k_9 = 5 \times 10^{-11}$ cm^3 molecule^{-1} s^{-1}.[27] However, from our experimental results, the effect of excessive NH_2 on the determination of the rate constant k_1 was negligible. A change of flash energy by a factor of 6 at 300 Torr should have changed $[NH_2]$ appreciably but had no effect on the k_1 measurement. Further investigation of the effect of NH_2 was carried out by replacing the flash lamp with a KrF excimer laser. The NH_3 photolysis was practically absent at 248 nm. The observed rates varied only within the experimental uncertainties of those determined with the Xe flash lamp. This result is also consistent with that reported by Smith and Zellner,[13] who placed NH_3 at

(27) Cheskis, S. G.; Sarkisov, O. M. *Chem. Phys. Lett.* **1979**, *62*, 72.

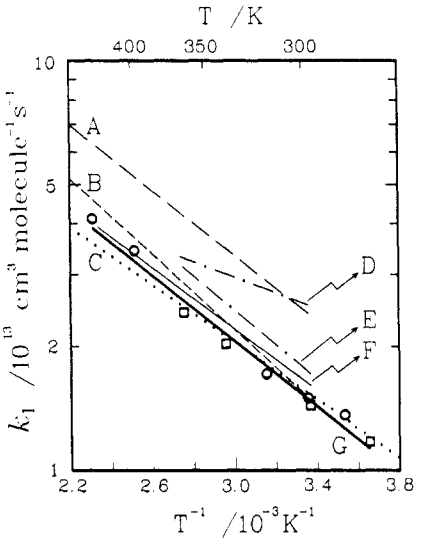

Figure 4. Arrhenius plot for the reaction OH + NH_3: A (– –), Hack et al.; B (- - -), Silver and Kolb; C (···), Smith and Zellner; D (–·–), Pagsberg et al.; E (·– –), Stephens; F (—), Perry et al.; G (▬), this work (□: Xe flash lamp photolysis; ○: KrF laser photolysis).

50–80 Torr before their flash lamp to reduce the NH_2 production but observed no variation in k_1. If one assumes a 10% upper limit for the contribution to the rate constant k_1 by interfering reaction 9, it is likely that k_9 has been overestimated and k_9 should be less than 7×10^{-12} cm^3 molecule^{-1} s^{-1}.

The observed rate constants at each temperature are shown in the Arrhenius plot, Figure 4. The results obtained from laser photolysis agree well with those from Xe flash photolysis. A fit to the Arrhenius equation by least squares yields

$$k_1 = (3.29 \pm 1.02) \times 10^{-12} \exp[-(922 \pm 100)/T] \quad \text{cm}^3\ \text{molecule}^{-1}\ \text{s}^{-1} \quad (10)$$

in which the uncertainties represent one standard error. This equation reproduces our experimental data within 8%.

Table II is a summary of the pertinent rate coefficients; because in this study we are concerned with the rate constants only at lower temperatures, the results for $T > 500$ K are omitted. The average of the rate constants determined at room temperature with the flash lamp and with the excimer laser, 1.47×10^{-13} cm^3 molecule^{-1} s^{-1}, is listed in Table II. This value is in excellent agreement with those reported by Stuhl,[8] Smith and Zellner,[13] Perry et al.,[14] Silver and Kolb,[17] and Stephens,[21] using either the flash photolysis or the discharge flow technique. The other reports are likely erroneous. As stated above, because in most previous flash photolysis studies there was no attempt to avoid the photolysis of NH_3, the agreement between those results and ours also indicates that unwanted photolysis did not interfere with measurements of the rate constants. Our experiments were carried out under more extensive conditions (to greater $[NH_3]$ and greater total pressure),

as indicated in Table II. The agreement in rate measurement also suggests that no apparent secondary reactions interfered with the measurements.

The reported Arrhenius equations are also illustrated in Figure 4 for comparison. The Arrhenius activation energy determined in this work, $E/R = 922 \pm 100$ K, is within the experimental uncertainties of those determined by Smith and Zellner,[13] Perry et al.,[14] Hack et al.,[10] and Stephens.[21] However, the rate constants reported by Hack et al.[10] are about 60% greater than the other four studies. The low E/R value, 438 ± 40 K, reported by Pagsberg et al.[15] is probably in error.

Although within experimental uncertainties, our data are mostly the smallest of the reported values. This may indicate that a small contribution from secondary reactions to the rate measurements was eliminated in our experiments. The rate constants actually showed a small positive deviation from the Arrhenius equation at higher temperatures, as illustrated in Figure 4. Jeffries and Smith[24] have proposed a modified three-parameter Arrhenius equation for reaction 1

$$k_1 = 1.58 \times 10^{-17} T^{1.8} \exp(-252/T) \quad \text{cm}^3 \text{ molecule}^{-1} \text{ s}^{-1} \quad (11)$$

which provides excellent fit to most data in the range $225 \leq T/\text{K} \leq 2350$. Our data are approximately 25% smaller than those predicted according to eq 11 at $T \leq 363$ K and 14% smaller at higher temperatures. This result suggests that the curvature of the Arrhenius plot is likely greater than that described in eq 11. However, because of the limited temperature range studied in this work, no attempt was made to derive an accurate expression of the modified Arrhenius equation from our data.

In conclusion, the rate of the reaction OH + NH_3 has been studied under extensive experimental conditions. Our data agree closely with those reported by Smith and Zellner.[13] The use of a KrF laser in photolysis eliminated the interference from excess NH_2. The agreement in the rate measurements by means of the Xe flash photolysis and the laser photolysis techniques indicates that the rate constant of the reaction OH + NH_2 is much smaller than the previous estimate.

Acknowledgment. We are grateful to the National Science Council of the Republic of China for the support of this research and to Dr. A. R. Ravishankara for helpful discussion and support.

Registry No. OH, 3352-57-6; NH_3, 7664-41-7; NH_2, 13770-40-6.

Collision-Theory Treatment of the Reactions of CH_3^+ with H_2, D_2, N_2, O_2, NO, CO, CO_2, HCN, and NH_3

L. F. Phillips

Chemistry Department, University of Canterbury, Christchurch, New Zealand *(Received: August 22, 1989; In Final Form: January 23, 1990)*

Rate constants have been calculated for bimolecular and, where appropriate, termolecular reactions in the presence of helium, neon, and argon bath gases, over the temperature range from 10 to 400 K. The contribution of the ion's rotational energy to the centrifugal barrier is included in all cases except the bimolecular reactions of CH_3^+ with H_2, D_2, and O_2. For the reaction of CH_3^+ with NO, the calculated capture rate is identical with the measured charge-transfer rate at 300 K. For collisions of CH_3R^+ complex ions with helium, inclusion of ion rotations causes the rate to be less than the Langevin rate by up to a factor of 3 at room temperature. From comparisons of calculated collision rates with experimental rate constants for association of CH_3^+ with HCN in the presence of He, Ne, Ar, and HCN, the same value of the collision efficiency β, namely 0.27 relative to HCN, is found for all three rare gases. For the reaction of CH_3^+ with NH_3, bimolecular and termolecular rate constants calculated with no adjustable parameters are in excellent accord with experimental data at 300 K.

Introduction

This paper gives the results of Langevin-type capture-rate calculations for a number of gas-phase reactions of CH_3^+ ions, and is concerned especially with predicting the temperature dependence of rate constants at the low-pressure limit. The present study gives no information about the pressure dependence of the rate constants, a topic which is being treated, for example, by RRKM-master equation calculations here and elsewhere.[1] Experimental values of room-temperature rate constants are available for all of the reactions considered, temperature dependences down to about 80 K have been measured for several of them,[2,3] and measurements of ion–molecule reaction rates at temperatures down to 10 K or less are in progress in at least two laboratories,[4,5] so that quite detailed comparisons between theory and experiment should soon be possible.

The calculations employ a recently developed computer program which performs approximate classical trajectory calculations to obtain rates of capture over the centrifugal barrier in a potential that can incorporate contributions from dipole–dipole, dipole–induced dipole, dipole–quadrupole, ion–dipole, ion–quadrupole, ion-polarization anisotropy ($\alpha_\parallel - \alpha_\perp$), ion–induced dipole, Morse, and London interactions.[6] Angle-dependent potentials are treated in a "frozen" approximation, which amounts to assuming that the probability of a collision occurring with a particular value of the angular factor in the potential does not vary during the progress of the collision (although the actual value of the angular factor may change as rotational motion of reactants is transformed into vibration at short range). For ion–molecule reactions, all angular factors are treated explicitly rather than by averaging $\cos^2\theta$ terms to 0.5. This is important for reactions of species with weak dipole moments, such as NO and CO, where the dominant angle-dependent interaction changes from ion–dipole at long range to ion–quadrupole at intermediate to short range. The algorithm normally conserves angular momentum by first forming a mean

(1) Smith, S. C.; McEwan, M. J.; Gilbert, R. G. *J. Chem. Phys.* **1989**, *90*, 1630, 4265.
(2) Anicich, V. G.; Huntress, Jr., W. T. *Astrophys. J. Suppl.* **1986**, *62*, 553.
(3) Ikazoe, Y.; Matsuoka, S.; Takebe, M.; Viggiano, A. *Gas-Phase Ion-Molecule Reaction Rate Constants Through 1986*; *Maruzen*: Tokyo, 1987.
(4) Rebrion, C.; Marquette, J. B.; Rowe, B.; Adams, N. G.; Smith, D. *Chem. Phys. Lett.* **1987**, *136*, 495.
(5) Randeniya, L. K; Zeng, X. K.; Smith, R. S.; Smith, M. A. *J. Phys. Chem.* **1989**, *93*, 8031.
(6) Phillips, L. F. *J. Comput Chem.* **1990**, *11*, 88.

0022-3654/90/2094-5265$02.50/0